The Fifth International Workshop on Micro and Nanotechnology for Power Generation and Energy Conversion Applications
PowerMEMS 2005
Nov. 28-30, 2005
Takeda Hall, The University of Tokyo, Tokyo, Japan

Experimental Development of the Rotating Subsystem for a Micro Rankine Power System

C. Lee[1], L. G. Fréchette[2,1]

[1] Columbia University – Dept. of Mech. Eng., 500 W. 120th St, New York, NY 10025, U.S.A.
[2] Université de Sherbrooke – Dept. of Mech. Eng., 2500 boul. Université, Sherbrooke, Québec J1K 2R1, Canada

Abstract

This paper presents de latest achievements in the development of a MicroTurboPump that includes a four stage radial microturbine, spiral groove seals, journal and thrust bearings, and a spiral groove viscous micropump. The device has been designed, fabricated and tested, as the core component of a MEMS-based Rankine cycle steam turbine power plant-on-a-chip. The fabrication challenges and realizations for the MicroTurboPump are presented, followed by the experimental characterization and test results achieved to date. The bearing and microturbine operation have been characterized at speeds above 300,000 RPM, and have found close agreement with modeling predictions. Results to date suggest that the proposed Rankine device should be a viable approach for micro power generation.

Keywords : Micro power generation, Microturbine, Micropump, Rankine cycle

1 - INTRODUCTION

Among the range of applications served by microelectromechanical system (MEMS) technology, *energy conversion* has received growing attention. Various power MEMS concepts, such as gas turbines, rocket engines, and internal combustion engines are in development to provide compact electric power sources and miniature propulsion units [1]. The concept pursued herein integrates in this thematic. It consists of a microturbine-based system that implements the Rankine vapor power cycle on a chip, aimed for compact power generation from a source of heat. This paper describes the most recent advances in development of the rotating subsystem, a core element of the Rankine device. Following a description of the micro Rankine power system, the rotating subsystem design, fabrication, and experimental characterization will be detailed.

1.1 - Micro Rankine Power System

The configuration of a complete micro Rankine power source consists of a heat source (burner with fuel tank or waste heat), a cooling mechanism (cooling fan or other heat removal approach), the MEMS-based micro Rankine device and power electronics. The Rankine device itself consists of a steam-driven turbine that entrains a liquid pump and a generator, along with an evaporator and a condenser, as illustrated in Figure 1. These components implement the Rankine power cycle, used in the vast majority of fossil-fueled or nuclear electrical power plants. The working fluid (water) is pressurized in liquid state, evaporated with the addition of heat from the external source, expanded through the turbine to provide mechanical power, and condensed back to liquid state. The proposed concept consists of miniaturizing and integrating the Rankine device using lithography, deep reactive ion etching, and aligned bonding of silicon and glass wafers (Figure 2). The device takes a planar form with dimensions on the order of 1cm^2 x 3 mm thick. Previous system-level studies suggest that an output electrical power of 1-12 W could be possible with overall energy conversion efficiencies ranging from 1-10% [4].

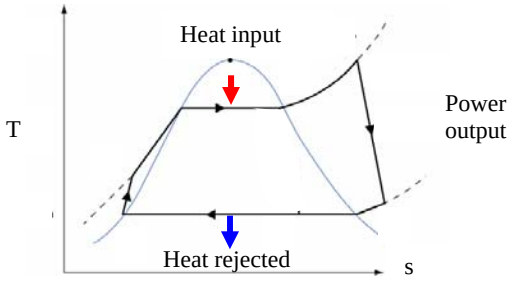

Figure 1 - Standard superheated Rankine power cycle, illustrated in a temperature-entropy diagram.

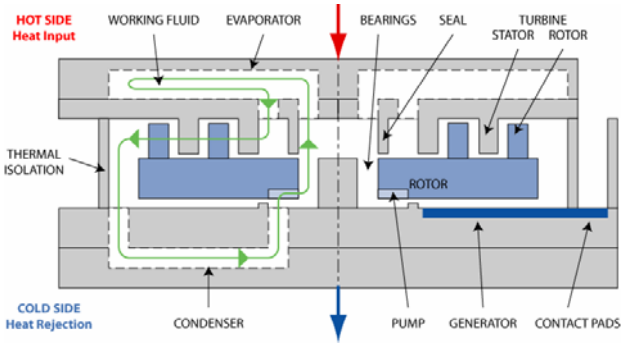

Figure 2 - Cross-section schematic of micro steam-turbine power plant-on-a-chip, constructed from 5 silicon wafers that are deep reactive ion etched and bonded to integrate the components on a single chip.

2 - ROTATING SUBSYSTEM: MICROTURBOPUMP

An incremental approach was adopted to develop the Rankine microsystem, as illustrated in Figure 3. The device was segregated in *thermal* and *rotating* subsystems, each developed with increasing levels of complexity.

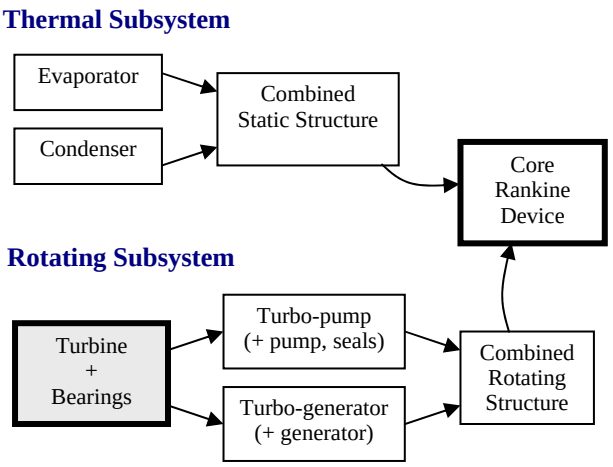

Figure 3 - Development approach for the Micro Rankine Power System.

The platform used to develop the rotating subsystem consists of a modular microturbopump that initially encloses a multistage microturbine, a spiral groove viscous pump, thrust and journal bearings, and seals (Figure 4). It is used to develop fabrication capabilities and validate the design principles and models for its components. The first experimental characterization effort focused on the turbine and bearing operation, and is the focus of this paper.

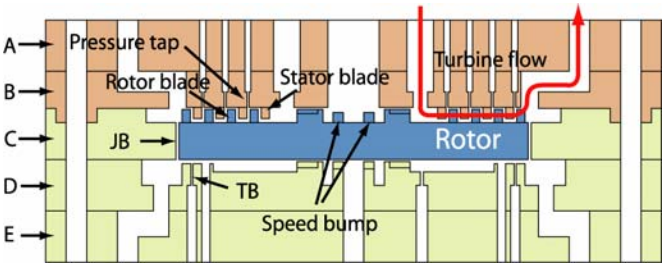

Figure 4 - Microturbopump device: a test bed for the development of the rotating components.

The overall configuration consists of five micromachined layers that enclose a 4 mm diameter rotor and form the flow paths to the bearings and turbine. The bearing system, which supports the rotor axially and laterally as it rotates, is composed of hydrostatic thrust and journal bearings. The rotor is a 4mm diameter disk with four concentric blade rows on one side, each composed of 80 to 180 blades. Four rows of stator blades also extend out from the upper layer, between the rotor blade rows, making an interdigitated radial flow turbine. The height of the rotor blades is 70um, and that of the stator blades is 50um.

As illustrated in Figure 4, the high pressure flow is fed from the top, does a right angle turn into the first blade row and flows outward through the turbine. Expansion of the working fluid provides the energy to drive the rotor. To replace the load that would result from the generator, a region of high viscous drag was intentionally added on the back side of the disk. This type of bearing system is directly inspired from previous microturbines [5]. The journal bearing, which is a circular trench of 20um wide and 400um deep, surrounds the rotor to support it radially. It exploits the boundary growth at the entrance of the narrow channel and difference of pressure distribution between opposite sides of the bearing to create a restoring force. The thrust bearing, which has a 1 um gap, is located on the bottom side of the rotor. It consists of 34 externally pressurized nozzles, which are 10 um diameter and 85 um long. It utilizes the flow resistances between nozzles and a planar clearance to balance out the axial movement of the rotor.

3 - MICROFABRICATION

The whole device chip set is composed of three pieces: top chip, bottom chip and rotor (Figure 5a). The top chip, which is the stack of layers A and B, has the turbine inlet and outlet flow channels and the stator blades. The rotor (Figure 5b) is a disk with four concentric rotor stages, a spiral groove seal, and protrusions ("speed bumps") to facilitate measurement of rotational speed. The bottom piece, which is the stack of layers C, D, and E, is the structure for the bearing system and related flow channels.

The 5 wafers are individually processed, then bonded to form the top and bottom chips. The rotor is fabricated as part of layer C and assembled manually before testing. The fabrication approach uses shallow silicon reactive ion etching (RIE) to create the recessed bearing surfaces, deep reactive ion etching (DRIE, Bosch process) to create the flow channels, turbine blades, journal bearing gap and thrust bearing nozzles. The fabrication process, illustrated in Figure 6, is as follows:

A-layer: On wafer #A, through holes are formed by ultrasonic drilling.

B-layer: A nested mask approach is used on the top side, consisting of a patterned SiO_2 film covered by a photoresist mask. A first DRIE is performed to form pressure ports, as defined by the photoresist mask. After removal of the photoresist, DRIE is pursued until the oxide layer is reached. Next, the opposite side is patterned and etched to the oxide layer. The exposed oxide is then removed by BOE to clear the through holes.

C-layer: The top side receives a shallow etch at first, followed by a deep etch to form the rotor blades. A 0.5 micron PECVD oxide is deposited to protect the surface before through etching. The journal bearing is etched from the bottom side, separating the rotors. A glass handle wafer was attached on the top side to prevent the rotors from falling in the chamber when etched. The rotors were finally released by removing the oxide layer and kept separately from the wafer.

D-layer: At first, the top side receives four shallow etches. Next, the bottom side is etched half way through, while the front side is covered with an oxide layer for surface protection. The top side is then patterned and etched until through holes are formed.

E-layer: The wafer is etched half way through from both sides to form channels and through holes.

A glass wafer was selected for layer A to allow visual observation of the rotor and the journal bearing. The stator is built from a silicon-on-insulator wafer (SOI) since the multistage turbine configuration requires interdigitated rotor and stator blade rows. Most of the 50 micron top silicon layer is etched, except for the stator blades and alignment features.

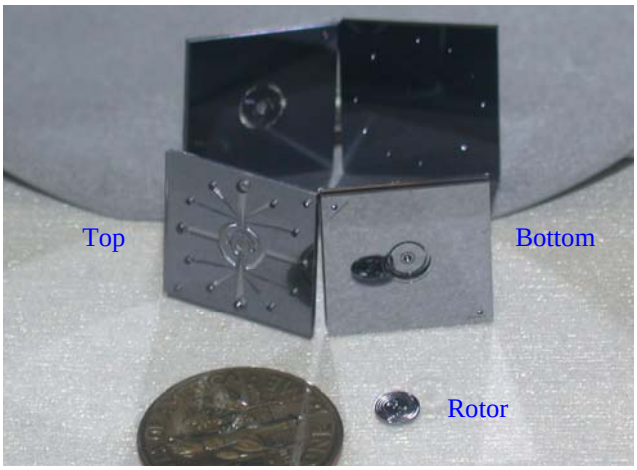

(a) Photograph of the completed microturbopump device, including the top chip (A-B), bottom chip (C-D-E), and rotor.

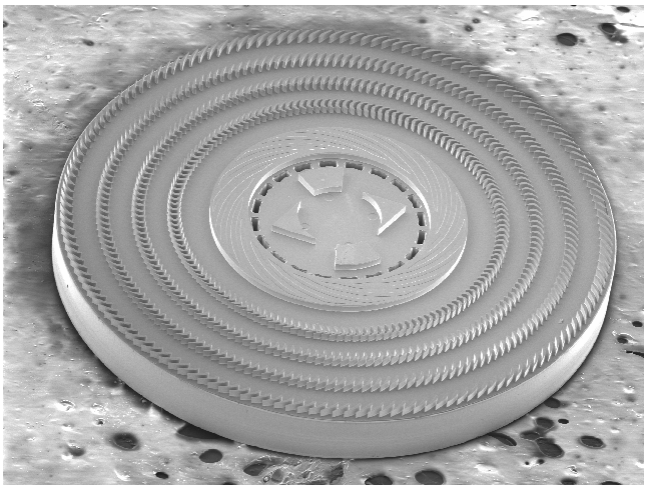

(b) SEM of a four stage microturbine rotor. The spiral groove seal is also visible, separating the return ports of the pump from the most inward turbine stage.

Figure 5 - Images of the completed MicroTurboPump device, showing the entire device (a) and a close-up of the rotor (b).

A-layer (glass wafer: Pyrex 7740)

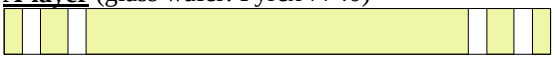

1) Ultrasonic through wafer drilling

B-layer (SOI wafer: 50 microns Si on 0.5 micron SiO_2)

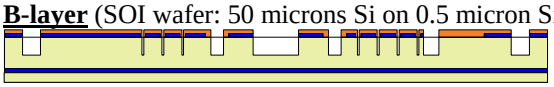

1) Create a nested mask, then DRIE 300 microns

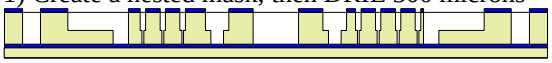

2) Remove PR, then DRIE 100 microns

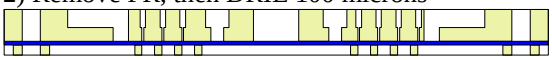

3) DRIE 50 microns and BOE to remove SiO_2

C-layer (Si)

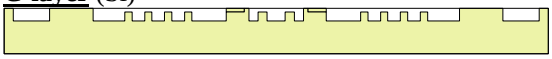

1) Shallow RIE 1.5micron, then DRIE 70 microns

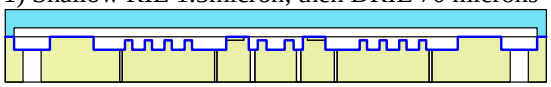

2) Mount on handle wafer and DRIE 400 microns

D-layer (Si)

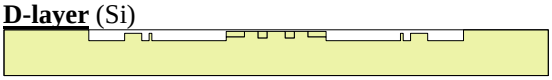

1) Shallow RIE (2, 0.5, 1.5, and 6 microns)

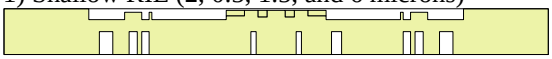

2) Deep etch from bottom side

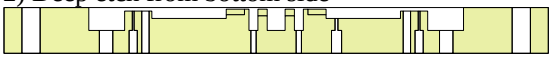

3) Deep etch from top side

E-layer (Si)

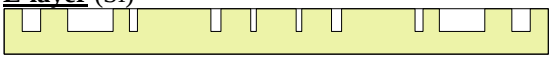

1) Deep etch halfway through from top side

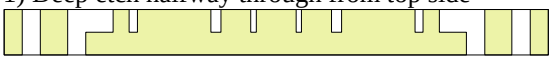

2) Deep etch from bottom side

Bonding

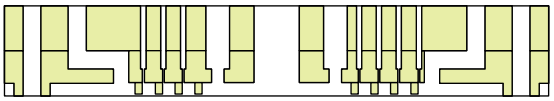

1) Anodic bonding of A and B layers

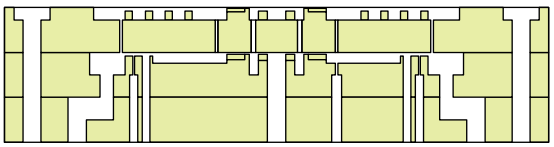

2) Fusion bonding of C, D, and E layers (without rotor)

Figure 6 - Fabrication process for the microturbopump, using one glass, one SOI, and three silicon wafers**.**

After the wafers are completed, they go through cleaning and aligned wafer-level bonding processes. The ultrasonically drilled glass wafer #A and deep etched silicon wafer #B were aligned and pressed with a slight force of 25N and remained in contact for 10 minutes in vacuum at 350 °C, with 1000 Volts applied. Wafers C, D, and E were aligned and the stack was pressed with a force of 1700N for 30 sec in vacuum. It was then annealed at 1000°C for 1 hour in a nitrogen environment.

4 - TESTING AND CHARACTERIZATION

For testing, the chips sets and rotors are manually assembled and clamped together with o-rings that simultaneously create the fluidic connections to the device. In this work, the device was operated with air instead of steam for simplicity. Flow rates or pressures were applied at the bearing and turbine ports using mass flow controllers and pressure sensors connected to a computer data acquisition system for monitoring and control. Rotational speed was measurement with a fiber optic reflectance probe aimed at the speed bumps on the rotor.

At first, the rotor was levitated by pressurizing the thrust bearing and applying a uniform pressure over the turbine side of the rotor. By varying the turbine-side pressure for a given thrust bearing pressure, the rotor was allowed to move axially. This displacement was measured with the optical probe and plotted in Figure 7. By estimating the axial force provided by the thrust bearing as being equal to the pressure force on the turbine side, the stiffness is found to be in the range of 0.1-0.3 N/μm. This test also confirms that the rotor was free to move axially and was not impeded to rotate due to the assembly approach.

By gradually introducing a pressure difference across the turbine inlet and outlet, flow was forced through the turbine and the rotor was spun. Results for two devices are presented in Figure 8. Rotational speeds up to 330,000 rpm were achieved in a stable and controlled fashion. Modeling results are superimposed, showing close agreement with our predictions (modeling details are beyond the scope of this paper). The maximum turbine power is calculated to be 0.38W.

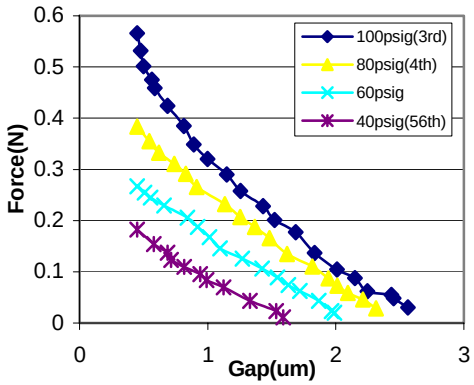

Figure 7 - Axial force of the hydrostatic thrust bearing as a function of thrust bearing gap. Each curve corresponds to a different thrust bearing supply pressure.

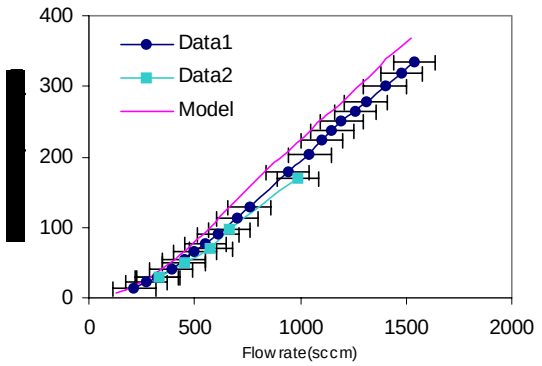

Figure 8 – Rotation rate as a function of air flow rate through the turbine. Data is presented for two different devices showing repeatability.

5 - CONCLUSIONS

The central building block of a Micro Rankine Power System, its rotating subsystem, has been designed, fabricated and initially tested up to high rotational speeds (330,000 rpm). This work demonstrates the feasibility of the fabrication approach for interdigitated microturbines as well as the design approach for the bearings and turbomachinery. On-going efforts consist of pursuing higher speed operation and characterizing the seals and pump. Pursuit of the path towards a functional Rankine power system will require significant research in the areas of two-phase flow micro heat exchanger, electromagnetic machinery, self-sustained bearings, and materials for high temperature operation.

ACKNOWLEDGMENTS

This work was supported by the NASA Glenn Research Center, Alternate Fuels Foundation Technologies program (contracts NAS3-02118 and NAS3-03105), monitored by Dr. Glenn Beheim. The authors gratefully acknowledge this support. The fabrication work was performed in part at the Cornell NanoScale Science and Technology Facility (CNF), a member of the National Nanotechnology Infrastructure Network, which is supported by the National Science Foundation (Grant ECS 03-35765).

REFERENCES

[1] Epstein, A.H., et al., "Micro-Heat Engines, Gas Turbines, and Rocket Engines - The MIT Microengine Project," AIAA Paper 97-1773, *28th AIAA Fluid Dynamics Conf.*, Snowmass Vil., 1997.

[2] Fu, K., *et al.*, 2001, "Design and Fabrication of a Silicon-Based MEMS Rotary Engine," *Proc. ASME Int'l Mech. Eng. Congress and Expo.*, New York, Nov. 11-16.

[3] Kang, P., Tanaka, S., and Esashi, M., "Demonstration of a MEMS-based turbocharger on a single rotor," *J. Micromech. Microeng.* Vol. 15, No 5, pp. 1076-1087, May 2005.

[4] Fréchette, L.G., Lee, C., Arslan, S., Liu, Y.-C., "Design of a Microfabricated Rankine Cycle Steam Turbine for Power Generation", *Proc. ASME Int'l Mech. Eng. Cong. & Expo.*, Wash., D.C., Nov. 16-21, 2003.

[5] Fréchette, L.G., et al., "High-Speed Microfabricated Silicon Turbomachinery and Fluid Film Bearings". *J. Microelectromech. Syst.* Vol. 14, No. 1, pp. 141-152, 2005.